V International Conference on Computational Methods for Coupled Problems in Science and Engineering
COUPLED PROBLEMS 2013
S. Idelsohn, M. Papadrakakis and B. Schrefler (Eds)

ON THE PERFORMANCE OF DETACHED-EDDY SIMULATION IN FLUID-STRUCTURE INTERACTION PROBLEMS

S. Türk*†, T. Reimann†, D.C. Sternel† and M. Schäfer†

*Graduate School of Computational Engineering
Technische Universität Darmstadt
Dolivostrasse 15, 64293 Darmstadt, Germany
e-mail: tuerk@gsc.tu-darmstadt.de, web page: http://www.graduate-school-ce.de/

†Institute of Numerical Methods in Mechanical Engineering
Technische Universität Darmstadt
Dolivostrasse 15, 64293 Darmstadt, Germany
web page: http://www.fnb.tu-darmstadt.de/

Key words: Hybrid Methods, Detached-Eddy Simulation, Fluid-Structure Interaction

Abstract. In this work a formulation for a ζ-f DES model has been used in its DES and URANS formulation to calculate the flow over an inclining plate in order to investigate the potential of DES on moving structures. It is shown that although the model is in LES mode, the fluctuations are not developed instantaneously. As a result, the turbulent kinetic energy is underpredicted in the LES zone, compared to pure URANS. The formulation for the ζ-f DES model has been validated for the flow over a streamwise periodic 2D hill, whereat the results are in good agreement to the available benchmark data obtained from LES.

1 INTRODUCTION

Although the computational power available has been rapidly increasing over the years, it is still not feasible to run Direct Numerical Simulations (DNS) or Large-Eddy Simulations (LES) for high Reynolds number problems at a reasonable computational cost. Thus, RANS Models are still the preferred method in a broad range of applications for practically relevant Reynolds numbers [12].
To overcome the lack of accuracy in pure RANS methods, several hybrid approaches, combining LES and RANS methods, were developed within several research groups. One of these hybrid techniques is the detached-eddy simulation (DES) first proposed by Spalart [13]. Motivated by the fact that a Large-eddy simulation of complete configurations such as an airplane or a wind-turbine is not feasible for the foreseeable future, the DES aims at

combining the favorable aspects of LES and RANS techniques, namely the application of RANS models for the calculation of attached boundary layers and the LES for resolving spatio-temporal fluctuations of large eddies.
In applications of massively separated flows, the geometry-specific structures cannot be well captured by the statistical models as those are calibrated for thin turbulent shear flows containing relatively "standard" eddies [17]. Despite the broad range of RANS models available and their capabilities to predict boundary layers and their separation well, those models fail at prediction of large separation regions behind a sphere, past a vehicle or an airfoil in deep stall. In addition no unsteady information can be gained from a RANS simulation leading to vibration or noise.
Contrary to the RANS approach, where turbulence is completely modeled, an LES would resolve the fluctuations in space and time down to small scales and only the very small scales are modeled by a subgrid-scale (SGS) model. Hence the demands on the grid spacing and the time step are very restrictive.
Especially in the context of fluid-structure interaction problems (FSI), the information on the vibration can be one major result of the whole calculation. Concerning the fact that in addition to the fluid dynamics, also the equations of motion for the structural part have to be solved per iteration, the problems become much more demanding in terms of computational cost. Thus, the use of DES in the context of FSI seems to be promising to account for the important unsteady information.
The potential of DES for turbulence modeling employed to FSI is mentioned in [17], while some experiences are described in [3]. A coupling between DES flow simulation and FEM data is reported in [8], where the fluid-structure interaction in the nozzle section of the Ariane 5 under transonic wind tunnel conditions is investigated. Another work [4] using DES for the FSI of a transonic rotor at near-stall conditions showed that with such a computational setup, the basic dynamic aeroelastic characteristics have been captured successfully.
It has been reported, that the influence of the underlying RANS model is minor on the overall result in the LES region [15]. However for more complex flow situations arising particularly from movable or deformable objects the impact of the model in the RANS region is observable, particularly if separation occurs and thus justifying the use of a more complex RANS.
Within this paper, a DES formulation for the ζ-f model by Hanjalic [6] is derived and validated with benchmark data from the flow over a streamwise periodic 2D hill. This formulation is then used to conduct a feasibility study for the use of DES in an FSI problem. A flat plate is inclined at a constant angular velocity of $\dot{\alpha} = \frac{10\pi}{3}\ \mathrm{rad\,s^{-1}}$ from 0° to 45° at a Reynolds number of $Re = 30000$. The simulations are carried out using DES [13] and DDES [16] on two different grids. We put focus on the dynamics with which fluctuations are generated and compare the results to pure URANS.

2 GOVERNING EQUATIONS

In the following an incompressible fluid with constant fluid properties is considered. For an incompressible Newtonian fluid, the flow has to satisfy the continuity and Navier-Stokes equations in the following form:

$$\frac{\partial u_i}{\partial x_i} = 0 \quad , \tag{1}$$

$$\rho \frac{Du_i}{Dt} = -\frac{\partial p}{\partial x_i} + \mu \frac{\partial^2 u_i}{\partial x_j^2} \quad . \tag{2}$$

where u_i is the velocity vector, p is the static pressure and μ is the dynamic viscosity. Using the Reynolds decomposition,

$$u(\mathbf{x}, t) = \overline{u(\mathbf{x})} + u'(\mathbf{x}, t) \quad , \tag{3}$$

where $\overline{u}$ is the mean motion and u' is the fluctuating component, the RANS equations can be derived from equation (2):

$$\frac{\partial \overline{u_i}}{\partial x_i} = 0 \quad , \tag{4}$$

$$\rho \frac{D\overline{u_i}}{Dt} = -\frac{\partial \overline{p}}{\partial x_i} + \mu \frac{\partial^2 \overline{u_i}}{\partial x_j^2} - \frac{\partial \overline{u_i' u_j'}}{\partial x_j} \quad . \tag{5}$$

Thus, equation (5) is the ensemble average of equation (2), where an additional term arises. This additional term describes the momentum transport due to turbulence motion causing a closure problem. Therefore, RANS turbulence models are used to model this new term. A detailed description of the RANS models used in this work can be found in [5] and [6].

3 MODELLING APPROACH

In the concept of detached-eddy simulations the computational domain is split into two parts, a RANS region and an LES region. In both cases the RANS turbulence model is either used as a normal turbulence model or used as a subgrid-scale (SGS) model for the LES mode, depending on the grid, the flow configuration and the location within the computational domain.
To modify a given RANS model to be used in DES, the dissipation term in the k-equation is replaced by an expression involving the turbulent length scale defined to

$$l_{turb} = min\left(l_{RANS}, C_{DES}\Delta\right) \quad , \tag{6}$$

where in the context of DES, Δ is specifically defined by $\Delta = max\left(\Delta_x, \Delta_y, \Delta_z\right)$ Thus, the length scale becomes the original RANS length scale ($l_{RANS} < C_{DES}\Delta$) or the length scale

for the SGS model ($l_{RANS} > C_{DES}\Delta$). For this method to be used together with low-Re turbulence models, an additional modification is necessary to eliminate the influence of the low-Re terms in the SGS mode. According to the concept introduced by Spalart [16], the DES length scale becomes

$$l_{DES} = C_{DES}\Delta\psi \quad , \tag{7}$$

where ψ is 1 for high-Re models and a function or a specific constant for low-Re models. The general idea of this ψ-function is based on the assumption that at equilibrium between the production and dissipation the RANS model in SGS mode should reduce to a Smagorinsky-like model, i.e. $\nu_t = (C\Delta)^2 S$, where C is a constant and S is the modulus of the mean rate-of-strain tensor. For further information on the derivation of the ψ-function see [16], [10]. The modified transport equation for the turbulent kinetic energy for the ζ-f model reads as

$$\rho\frac{Dk}{Dt} = \frac{\partial}{\partial x_j}\left[\left(\mu + \frac{\mu_t}{\sigma_k}\right)\frac{\partial k}{\partial x_j}\right] + P_k - \rho\frac{k^{3/2}}{l_{turb}} \quad . \tag{8}$$

The corresponding ψ-function is derived as

$$\psi = \sqrt{\left(\frac{C_{\epsilon 1}}{C_{\epsilon 2}C_\mu\zeta}\right)^{3/2}} \quad . \tag{9}$$

The ζ-f model used in this work is also used in a DES context in [1]. However, the ψ-functions derived are different but both plausible. The constant C_{DES} is calibrated using Decay of Isotropic Turbulence (DIT) to account for the different underlying turbulence models but also for the numerical schemes that are used. For the calibration two different grids, consisting of 32^3 and 64^3 grid points are used. The field is initialized with the data from [22] and the results are also compared to the DNS data from Wray [22]. For detailed description of the procedure, see [10]. For the 3D Fourier transform a tool written by St. Petersburg Technical University (SPTU) is used. In this work C_{DES} is calibrated to

$$C_{DES} = 0.2 \quad . \tag{10}$$

Due to some drawbacks of the original DES formulation from equation (6) which we will refer to as DES97 through out this paper, a modified version was suggested by Spalart [16] named DDES. In order to preserve RANS mode in the boundary layer also on grids where the wall parallel spacing is smaller than the turbulent length scale, causing a switch to LES mode, a blending function is introduced. The blending function limits the LES mode to regions outside the boundary layer. For the DDES, the formulation reads:

$$r_d = \frac{\nu_t + \nu}{\sqrt{U_{i,j}U_{i,j}\kappa^2 d^2}} \quad , \tag{11}$$

where ν_t is the kinematic eddy viscosity, ν is the molecular viscosity, $U_{i,j}$ are the velocity gradients, κ is the Kármán constant and d is the wall distance. The quantity r_d is then used in

$$f_d = 1 - \tanh\left([8r_d]^3\right) \tag{12}$$

in such a way that f_d is one in the LES region and zero elsewhere. Therefore, the DES length scale is re-defined as:

$$l_{DDES} = l_{RANS} - f_d \; max(0, d - C_{DES}\Delta\psi) \quad . \tag{13}$$

4 NUMERICAL CONDITIONS AND METHODS

In the present work a Detached-Eddy Simulation is performed for a flat plate changing its angle of attack from 0°to 45°at a rotational speed of

$$\dot{\alpha} = \frac{10\pi}{3} \; \frac{rad}{s} \quad .$$

To avoid discontinuities in the angular motion, the following expression is used to describe the motion of the plate:

$$\alpha(t) = \frac{\pi}{4}\left[sin\left(\frac{\pi}{T}t\right)\right]^2 \quad ,$$

where $T = 0.15$ s is one period. Thus, for a motion from 0°to 45°, only $T/2$ is considered. The reduced pitching frequency for a non periodic motion is defined to $k_{pitch} = \Delta\ \alpha c/(U_b \Delta t) = 0.168$, where $U_b = 3.75\ \mathrm{m\,s^{-1}}$ is the bulk velocity at the inlet. The applied boundary conditions and the computational domain are shown in figure 1, where x,y and z correspond to the streamwise, spanwise and wall-normal direction respectively. At top and bottom of the computational domain no-slip boundary conditions are applied as well as on the plate, located in the center. In spanwise direction, periodic boundary conditions are used. On the inlet plane, a profile of a fully developed turbulent channel flow without any perturbations is applied while on the outlet plane a zero gradient boundary condition is used. The size of the computational domain is chosen according to the future experimental setup, where the measurements are taken in a square channel of a cross section of 0.45×0.45 m^2 and a length of 2 m. The chord length is $c = 0.12$ m^2 and the Aspect Ratio is $AR = 3.67$. The thickness is 0.006 m^2.
In the computational setup only two chord lengths in spanwise direction are resolved in order to reduce the computational cost, which can be justified by the two-dimensional character of the experimental setup. Due to the fact that the trailing edge of the plate is moving towards the bottom wall, top and bottom walls are resolved in the simulation. In this study two different grids were used to evaluate the influence of the grid on the performance of the DES. A summary of the two grids is given in table 1. Both grids are built following the guidelines given in [14]. To ensure the grid quality in the region around the plate, where the vortex shedding and recirculation is expected, the O-Grid blocks are rotated with the plate. Thus, no re-meshing or grid generation method is needed in the

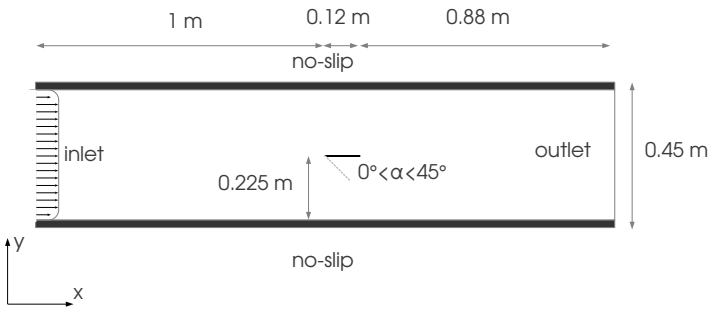

Figure 1: Sketch of computational domain

Table 1: General grid information for the simulations performed

Total No. of CVs	CVs in circumferential direction of the plate	CVs in spanwise direction per chord length	Wall normal grid spacing
2.2×10^6	136	16	$y^+_{max} < 1$
2.6×10^6	240	32	$y^+_{max} < 1$

region of interest leading to a decrease in the computational cost.
We use the finite volume solver FASTEST [18] with block structured, boundary fitted grids. The convective and diffusive fluxes are approximated with second-order central difference schemes in the LES mode and with the GAMMA [7] scheme in RANS mode. The blending between CDS and GAMMA is done by a blending function introduced in [20]. For the time discretization, we use a backward differencing scheme with second order accuracy and the coupling between pressure and velocity is done with the SIMPLE algorithm. The parallelization in FASTEST is done via domain decomposition using MPI.

5 RESULTS AND DISCUSSION

5.1 Flow over streamwise periodic 2D hill

To validate the DES formulation for the ζ-f model [6], the flow over a streamwise periodic 2D hill for a Reynolds number of $Re_b \approx 10600$ is calculated and compared to benchmark data. This benchmark scenario has already been investigated for DES in several studies, for example [11] and [21]. The geometry here is the same as in [19] and the results are compared to the benchmark LES from Temmerman and Leschziner [19], serving as the standard reference data. All quantities are nondimensionalized by the hill

height h and the bulk velocity at the hill crest, U_b. The results are averaged in time and spanwise direction. The time step was chosen so that $CFL_{max} \approx 1$ to ensure the temporal resolution, while the effect of higher CFL numbers is reported in [11]. The domain is discretized by approximately 1.7×10^6 control volumes, while the wall distance of the first grid point is about $y^+ \approx 0.5$.
The velocity profiles as well as the $\overline{u'v'}$ component of the Reynolds stress tensor, shown in figure 2, are in good agreement with the benchmark LES. The separation point is located at $x/h = 0.14$ while the flow reattaches at $x/h = 4.6$, whereas the reference points in [19] are at $x/h = 0.22$ and $x/h = 4.72$ respectively. Thus, both points are slightly shifted towards the crest of the hill.

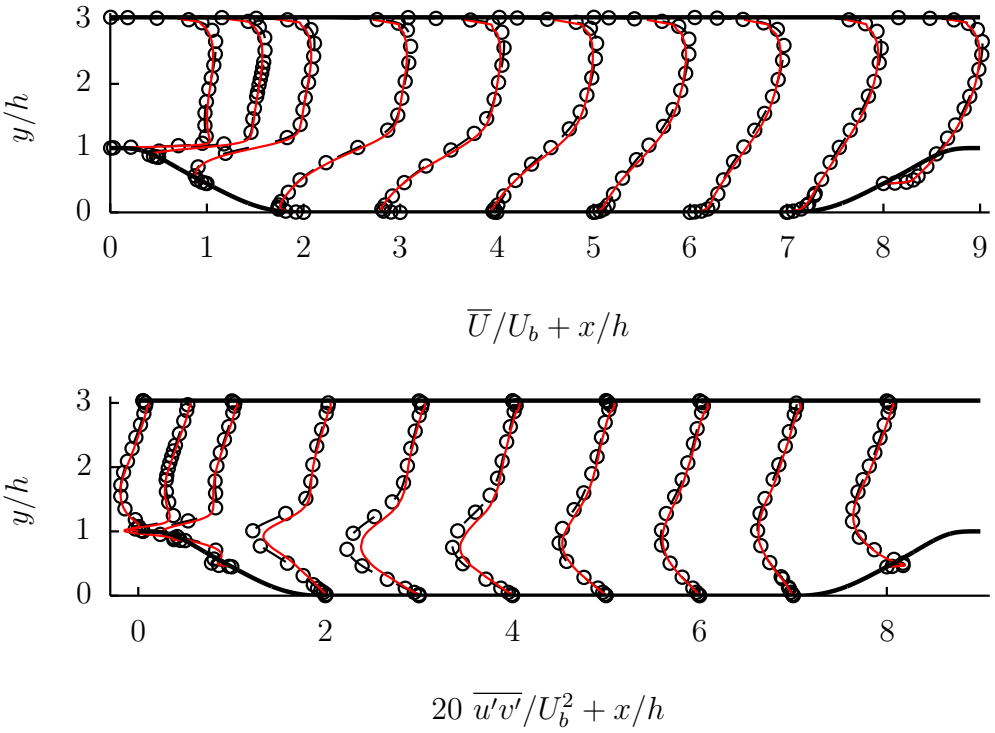

Figure 2: Validation of $\overline{U}$ and $\overline{u'v'}$ at reference locations, $^-\circ^-$ DES97, — LES from [19]

5.2 Flow over an inclining plate

The main objective of this work is the further investigation of DES methods in the context of FSI focused on the generation of fluctuations for rapidly moving structures. For the given inflow conditions, the flow field does not contain any fluctuations at the beginning, but a vortex street behind the plate at zero angle of attack is developed resulting in the formation of a small LES region, including fluctuations. For the DDES test cases,

Table 2: Overview of the simulations performed

Abbreviation	DES mode	SGS/RANS model	grid
ddes–f	DDES	ζ-f	fine
des97-f	DES97	k-ζ-f	fine
ddes-c	DDES	ζ-f	coarse
rans-f	RANS	ζ-f	fine

the major part of the computational domain is treated in RANS mode. For the DES97, almost in the entire region in front and around the plate, the RANS model is operating as an SGS model but not creating any fluctuations.
Consequently the turbulent viscosity, turbulent kinetic energy and the dissipation is reduced in the DES97 case. However, the velocity profile does not alter significantly downstream up to the plate, which might be attributed to the chosen boundary conditions at in and outlet. The log-layer mismatch observed in periodic channel flows is not found here.
In the upstroke phase ($0 < \alpha < 45°$), all configurations in table 2 predict a similar shape for the lift coefficient, C_L, and the drag coefficient, C_D, as shown in figure 3. No significant difference between RANS and DES can be detected but the grid refinement shows some influence on the results. For all cases no outstanding fluctuations are generated and the flow has a strongly two-dimensional character. This two dimensional behavior in the upstroke phase is also observed by Martinat et al. [9], where the flow past a pitching airfoil is investigated. For the downstroke phase on the other hand, they reported a reinforced adverse pressure gradient leading to a highly three dimensional flow. In the present work, this downstroke phase is excluded and thus not reinforcing three dimensional patterns. The LES zone is initialized at the lee side and consequently resulting in a reduced modeled turbulent kinetic energy, turbulent viscosity and dissipation, compared to URANS.
Once the plate remains at a constant angle of attack of $\alpha = 45°$, fluctuations start to generate and become more dominant over time but not as much as expected. A deviation in C_L and C_D starts evolve for $2t/T > 1.5$. Comparing the velocity field and the corresponding streamlines at $2t/T = 1.8$ in figure 4, the vortex at the trailing edge is still pinned to the plate for the ddes-f and ddes-c case, whereas the vortex is already shed in the other two configurations. For the coarser grid, only one big and flat vortex at the leading edge is resolved compared to the fine grid. For the DDES cases the LES zones is growing in time but the resolved fluctuations are not developed in a large number. However, for a pure URANS simulation resolving the spanwise direction the flow field presented in figure 5 shows the most turbulent fluctuations of all cases considered and does not converge to a steady state. Comparing the modeled turbulent kinetic energy, shown in figure 6, it becomes clear that the modeled contribution is reduced in the LES region while at the same time, fluctuations have not been developed yet as illustrated in

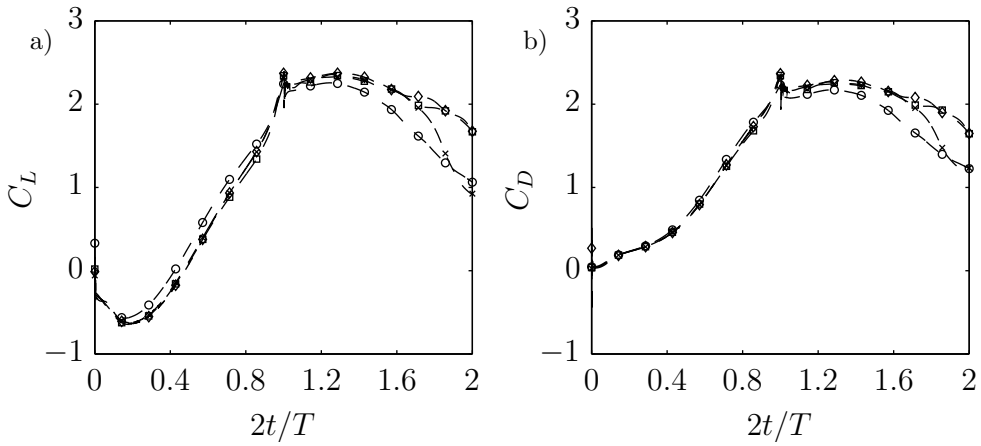

Figure 3: Lift Coefficient over T/2. ◇ des97-f, × ddes-f, □ rans-f, ○ ddes-c

figure 5, leading to an underprediction of the total turbulent kinetic energy as opposed to URANS. Against expectation the DES97 case does not develop an LES Zone comparable to the DDES cases and thus treating almost the entire lee side in RANS mode, which explains the good agreement between des97-f and rans-f in terms of C_L and C_D.
Simulating further in time, the problem then results in the case of a flat plate at high incidence which has been investigated by Breuer et al. [2], who showed the capability of DES in that specific flow situation, but is out of focus in this work. The fluctuations are then clearly detectable also in our case.

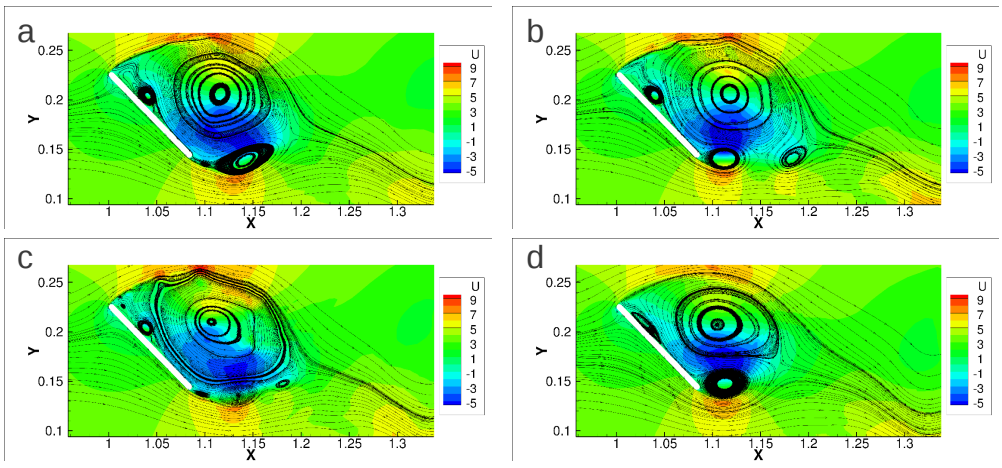

Figure 4: Contour of streamwise velocity component, averaged in spanwise direction including streamlines at $2t/T = 1.8$. a) des97-f, b) ddes-f, c) rans-f, d) ddes-c

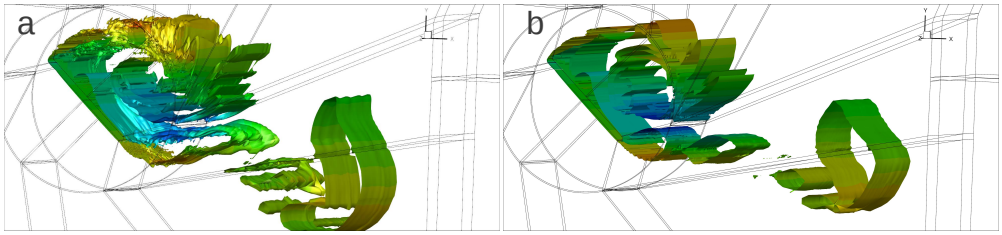

Figure 5: Isosurfaces of vorticity magnitude, colored by streamwise velocity at $2t/T = 1.8$. a) rans-f, b) ddes-f

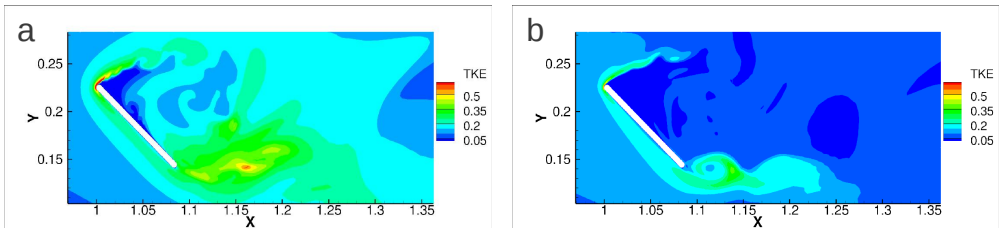

Figure 6: Contour plot of modeled turbulent kinetic energy at $2t/T = 1.8$. a) rans-f, b) ddes-f

6 CONCLUSIONS

We derived a DES formulation for the ζ-f model by Hanjalic [6] and validated the expressions with the benchmark data from [19] for a streamwise periodic 2D hill. The results are in good agreement with the LES data. Furthermore it is shown that the use of DES97 and DDES is not advantageous over URANS for a ramping plate without separation at the beginning. Future work will be dealing with the investigation of IDDES for the rapidly inclining plate, which is promising in terms of missing fluctuations, as the region upstream of the plate should already contain those fluctuations, arsing from the WMLES branch of IDDES. Additionally the results will be compared to experiments to perform a quantitative analysis. The simulations will also be repeated for the oscillatory motion.

7 AFFILIATION

This work is supported by the 'Excellence Initiative' of the German Federal and State Governments and the Graduate School of Computational Engineering at Technische Universität Darmstadt.

REFERENCES

[1] N. Ashton, R. Prosser, and A. Revell. A hybrid numerical scheme for a new formulation of delayed detached-eddy simulation (DDES) based on elliptic relaxation. *Journal of Physics: Conference Series*, 318(4):042043, December 2011.

[2] M. Breuer, N. Jovii, and K. Mazaev. Comparison of DES, RANS and LES for the separated flow around a flat plate at high incidence. *International Journal for Numerical Methods in Fluids*, 41(4):357388, 2003.

[3] U. Bunge. *Numerische Simulation turbulenter Strömungen im Kontext der Wechselwirkung zwischen Fluid und Struktur*. Univ.-Verlag der TU, Univ.-Bibliothek, 2005.

[4] X. Chen, H. Im, and G.-C. Zha. Fully coupled fluid-structural interaction of a transonic rotor at near-stall conditions using detached eddy simulation. American Institute of Aeronautics and Astronautics, January 2011.

[5] K-Y Chien. Predictions of channel and boundary-layer flows with a low-reynolds-number turbulence model. *AIAA Journal*, 20(1):33–38, January 1982.

[6] K. Hanjali, M. Popovac, and M. Hadiabdi. A robust near-wall elliptic-relaxation eddy-viscosity turbulence model for CFD. *International Journal of Heat and Fluid Flow*, 25(6):1047–1051, December 2004.

[7] H. Jasak, H. Weller, and A. Gosman. High resolution NVD differencing scheme for arbitrarily unstructured meshes. *International Journal for Numerical Methods in Fluids*, 31(2):431449, 1999.

[8] Heinrich Lüdeke, Javier B Calvo, and Alexander Filimon. Fluid structure interaction at the ariane-5 nozzle section by advanced turbulence models. In *European Conference on Computational Fluid Dynamics ECCOMAS CFD*, 2006.

[9] G. Martinat, M. Braza, Y. Hoarau, and G. Harran. Turbulence modelling of the flow past a pitching NACA0012 airfoil at and reynolds numbers. *Journal of Fluids and Structures*, 24(8):1294–1303, November 2008.

[10] C. Mockett. *A Comprehensive Study of Detached-Eddy Simulation*. Univ.-Verlag der TU, Univ.-Bibliothek, 2009.

[11] C. Mockett, M. Fuchs, and F. Thiele. Progress in DES for wall-modelled LES of complex internal flows. *Computers & Fluids*, 65:44–55, July 2012.

[12] P. Spalart. Reflections on RANS modelling. In Shia-Hui Peng, Piotr Doerffer, and Werner Haase, editors, *Progress in Hybrid RANS-LES Modelling*, number 111 in Notes on Numerical Fluid Mechanics and Multidisciplinary Design, pages 7–24. Springer Berlin Heidelberg, January 2010.

[13] P. Spalart, W. Jou, M. Strelets, and S. Allmaras. Comments of feasibility of LES for wings, and on a hybrid RANS/LES approach. In *International Conference on DNS/LES, Aug. 4-8, 1997, Ruston, Louisiana.*, 1997.

[14] P. R. Spalart. Young-persons guide to detached-eddy simulation grids. Technical report, NASA Langley Technical Report Server, 2001.

[15] P. R. Spalart. Detached-eddy simulation. *Annual Review of Fluid Mechanics*, 41(1):181–202, 2009.

[16] P. R. Spalart, S. Deck, M. L. Shur, K. D. Squires, M. Kh Strelets, and A. Travin. A new version of detached-eddy simulation, resistant to ambiguous grid densities. *Theoretical and Computational Fluid Dynamics*, 20(3):181–195, July 2006.

[17] K. D. Squires. Detached-eddy simulation: Current status and perspectives. *Direct and Large-Eddy Simulation V*, pages 465–480, 2004.

[18] D. C. Sternel. FASTEST-Manual, 2005.

[19] L. Temmerman and M. Leschziner. Large eddy simulation of separated flow in a streamwise periodic channel constriction. In *Int. Symp. on Turbulence and Shear Flow Phenomena*, pages 27–29, Stockholm, 2001.

[20] A. Travin, M. Shur, M. Strelets, and P. R. Spalart. Physical and numerical upgrades in the detached-eddy simulation of complex turbulent flows. In R. Friedrich and W. Rodi, editors, *Advances in LES of Complex Flows*, number 65 in Fluid Mechanics and Its Applications, pages 239–254. Springer Netherlands, January 2004.

[21] S. Šarić, S. Jakirlić, M. Breuer, B. Jaffrézic, G. Deng, O. Chikhaoui, J. Fröhlich, D. von Terzi, M. Manhart, and N. Peller. Evaluation of detached eddy simulations for predicting the flow over periodic hills. *ESAIM: Proceedings*, 16:133–145, March 2007.

[22] AA Wray. A selection of test cases for the validation of large-eddy simulations of turbulent flows. *AGARD Advisory Report*, 345, 1998.